



# Changes in coral reef community structure in response to year-long incubations under contrasting $p\text{CO}_2$ regimes

Peter J. Edmunds<sup>1</sup> · Steve S. Doo<sup>1</sup> · Robert C. Carpenter<sup>1</sup>

Received: 4 January 2019 / Accepted: 4 June 2019 / Published online: 17 June 2019  
© Springer-Verlag GmbH Germany, part of Springer Nature 2019

## Abstract

Coral reefs are threatened by ocean acidification (OA), which depresses net calcification of corals, calcified algae, and coral reef communities. These effects have been quantified for many organisms, but most experiments last weeks-to-months, and do not test for effects on community structure. Here, the effects of OA on back reef communities from Mo'orea, French Polynesia (17.492 S, 149.826 W), were tested from 12 November 2015 to 16 November 2016 in outdoor flumes maintained at mean  $p\text{CO}_2$  levels of 364  $\mu\text{atm}$ , 564  $\mu\text{atm}$ , 761  $\mu\text{atm}$ , and 1067  $\mu\text{atm}$ . The communities consisted of four corals and two calcified algae, with change in mass ( $G_{\text{net}}$ , a combination of gross accretion and dissolution) and percent cover recorded monthly. For massive *Porites* and *Montipora* spp.,  $G_{\text{net}}$  differed among treatments, and at 1067  $\mu\text{atm}$  (relative to ambient) was reduced and still positive; for *Porolithon onkodes*, all of which died,  $G_{\text{net}}$  was negative at high  $p\text{CO}_2$ , revealing dissolution (sample sizes were too small for analysis of  $G_{\text{net}}$  for other taxa). Growth rates (% cover month<sup>-1</sup>) were unaffected by  $p\text{CO}_2$  for *Montipora* spp., *P. rus*, *Pocillopora verrucosa*, and *Lithophyllum kotschyannum*, but were depressed for massive *Porites* at 564  $\mu\text{atm}$ . Multivariate community structure changed among seasons, and the variation under all elevated  $p\text{CO}_2$  treatments differed from that recorded at 364  $\mu\text{atm}$ , and was greatest under 564  $\mu\text{atm}$  and 761  $\mu\text{atm}$   $p\text{CO}_2$ . Temporal variation in multivariate community structure could not be attributed solely to the effects of OA on the chemical and physical properties of seawater. Together, these results suggest that coral reef community structure may be more resilient to OA than suggested by the negative effects of high  $p\text{CO}_2$  on  $G_{\text{net}}$  of their component organisms.

## Introduction

The physiological responses of coral reefs and reef organisms to ocean acidification (OA) are relatively well known (Kroeker et al. 2010; Chan and Connolly 2012). For scleractinian corals, calcification is expected to decline ~15% per unit reduction in aragonite saturation state ( $\Omega_{\text{arag}}$ , for  $2 < \Omega_{\text{arag}} < 4$ ) (Chan and Connolly 2012), and for calcified algae, ~0–8% per unit decline in calcite saturation state

from ambient values (Kroeker et al. 2013; Comeau et al. 2014). There is variation among taxa and functional groups in the sensitivity of calcification to  $p\text{CO}_2$  (Kroeker et al. 2013; Comeau et al. 2014), which indicates that community structure will modulate effects of OA on net community calcification. While this conclusion is supported by studies of coral reefs naturally enriched with  $\text{CO}_2$  (Fabricius et al. 2011), analyses of coral reef communities incubated for weeks under high  $p\text{CO}_2$  reveal negative effects on net calcification that are driven by dissolution of sediments and carbonate rock rather than calcification (Dove et al. 2013; Comeau et al. 2016).

Despite advances in understanding the effects of OA on the net calcification of coral reefs (Comeau et al. 2016; Albright et al. 2018), little is known of the effects on community structure. This omission makes it challenging to couple research describing the effects of OA on coral reefs with ecological analyses of their community structure. Two studies have experimentally addressed the effects of OA on coral communities for > 2 months (Langdon et al. 2000; Dove et al. 2013), and community structure was addressed

---

Responsible Editor: C. Voolstra.

---

Reviewed by Y. Sawall and an undisclosed expert.

---

**Electronic supplementary material** The online version of this article (<https://doi.org/10.1007/s00227-019-3540-2>) contains supplementary material, which is available to authorized users.

---

✉ Peter J. Edmunds  
peter.edmunds@csun.edu

<sup>1</sup> Department of Biology, California State University, 18111 Nordhoff Street, Northridge, CA 91330-8303, USA

in one study; two mensurative tests of the effects of  $p\text{CO}_2$  on coral communities have been conducted (Fabricius et al. 2011, 2014). Dove et al. (2013) incubated coral reef communities in 300-L tanks under four  $p\text{CO}_2$  regimes, and created communities simulating bommies at 5-m depth on Heron Island, Australia. Their experiment began with 35% coral, 15% macroalgae, and 48% sand, and after ~84 days, net calcification ranged from  $+5.3 \text{ g m}^{-2} \text{ h}^{-1}$  (301  $\mu\text{atm}$ ) to  $-3.8 \text{ g m}^{-2} \text{ h}^{-1}$  (1009  $\mu\text{atm}$ ), and coral cover declined 11% (301 and 405  $\mu\text{atm}$ ) or 30% (611 and 1009  $\mu\text{atm}$ ).

The present study tested the effects of OA on coral reef communities that were assembled with organisms from the back reef of Mo'orea, French Polynesia, and incubated for a year under different  $p\text{CO}_2$  treatments. We embraced the complexities of medium-volume ( $10^2$ – $10^4$  L) mesocosms operated over medium time scales (1 month–1 year; Stewart et al. 2013), and focused on community structure as an emergent property of organismic processes. An advantage of this approach is the ecological relevance attained from working with communities exposed to treatments for a long period relative to the speed with which organisms acclimatize (Somero 2015). Despite this advantage, there are limitations of mesocosms, notably in the potential for “random walks” from initial conditions (Stewart et al. 2013), and their high costs. Nevertheless, mesocosms provide important insights to the response of communities to environmental conditions, especially when placed in a context of experimental analyses conducted on a variety of functional and temporal scales. Our results focus on the community response to  $p\text{CO}_2$ , but we describe the effects on organism mass (i.e., net calcification,  $G_{\text{net}}$ ) to supplement the interpretation. We address the response of  $G_{\text{net}}$  to  $p\text{CO}_2$ , and then test the null hypotheses that: (1) the changes in planar area of corals and algae are unaffected by  $p\text{CO}_2$ , (2) benthic community structure (i.e., variation in the abundance of members of each taxon as measured by planar area) is unaffected by  $p\text{CO}_2$ , and (3) changes in community structure are independent of the physical and chemical features of seawater.

## Methods

**Overview** Back reef communities were assembled in four flumes (Fig. S1), with each randomly assigned to  $p\text{CO}_2$  treatments targeting ambient (400  $\mu\text{atm}$ ), 700  $\mu\text{atm}$ , 1000  $\mu\text{atm}$ , and 1300  $\mu\text{atm}$   $p\text{CO}_2$  to approximate atmospheric  $p\text{CO}_2$  projected for ~2140 under representative concentration pathways (RCP) 2.6, 4.5, 6.0 and 8.5, respectively (IPCC 2014). Treatments were maintained for 1 year from November 2015, and actual  $p\text{CO}_2$  treatments differed from target values. Each flume consisted of a working section that was 5.0 m long, 30 cm wide and filled to ~30-cm depth with ~500 L of seawater that was circulated and refreshed

with sand-filtered (pore size ~450–550  $\mu\text{m}$ ) seawater from Cook's Bay (14-m depth) at ~5  $\text{L min}^{-1}$  (Carpenter et al. 2018).

Planar growth and community structure were measured because they are used in ecological analyses of coral reefs, and we reasoned they would sharpen the ability to interpret the ecological implications of the physiological impacts of OA on calcification (Chan and Connolly 2012; Kornder et al. 2018). We anticipated that the community response to OA would include reduced linear extension, impaired planar growth of tissue and skeleton, and increase partial mortality (as in Dove et al. 2013). The mean linear extension expected for the corals in the present study (*Porites rus* =  $15.2 \pm 5.7 \text{ mm year}^{-1}$ , massive *Porites* =  $10.0 \pm 0.6 \text{ mm year}^{-1}$ , *Montipora* =  $27.7 + 3.0 \text{ mm year}^{-1}$ , and *Pocillopora verrucosa* =  $24.7 \pm 2.4 \text{ mm y}^{-1}$  [<https://coraltraits.org/>, accessed 8 October 2018]) were expected to create annual changes in planar area of 52  $\text{cm}^2$  (with mean initial size of 69  $\text{cm}^2$ ), 32  $\text{cm}^2$  (with mean initial size of 68  $\text{cm}^2$ ), 106  $\text{cm}^2$  (with mean initial size of 70  $\text{cm}^2$ ), and 150  $\text{cm}^2$  (with mean initial size of 218  $\text{cm}^2$ ), respectively, in the ambient flume. To evaluate the precision of the photographic method, 10 independent images of mounding and branching corals in the flumes were recorded, and were processed to provide replicate determinations of organism size (i.e., planar area). These images showed that the standard deviations of mean area determinations were 2.3% for massive *Porites*, and 3.8% for *P. verrucosa*. Based on these measures of precision, there would be a 75% chance of detecting annual growth of 0.6  $\text{cm}^2$  for massive *Porites* and 4.8  $\text{cm}^2$  for *P. verrucosa* (with  $n=4$ ), which represent reasonable estimates for the growth of these corals in our flumes (Carpenter et al. 2018). Given effect sizes ranging from 21.1% for *Lithophyllum* to 10.2% for massive *Porites* upon exposure to 1067  $\mu\text{atm}$   $p\text{CO}_2$  (Comeau et al. 2014), an effect of  $p\text{CO}_2$  on growth in the present study would be detectable for *Montipora*, while smaller effects of  $p\text{CO}_2$  for other taxa might be prone to Type II errors in detection (i.e., they might not be detected when present).

**Back reef communities** Back reef communities were assembled to correspond to the mean percent cover of the major space holders in this habitat in 2013 (data archived in Edmunds 2015). The communities began with ~25% coral cover, with 11% massive *Porites* spp., 7% *Porites rus*, 4% *Montipora* spp., 3% *Pocillopora* spp., and ~7% crustose coralline algae (CCA), consisting of 4% *Porolithon onkodes* and 3% *Lithophyllum kotschyannum*. Coral rubble (~1-cm diameter) was added to ~5% cover, and the remainder of the benthic surface was sand. Analyses of community structure focused on the central, 2.4-m long portion of this community where corals and CCA were secured to a plastic-coated, metal grid (5 × 5 cm mesh) and represented the “fixed” community (Fig. S1). Securing organisms to the grid was critical

to reduce parallax errors in photography, to allow the organisms to grow and interact as they extended over the year experiment, and to allow ecologically meaningful analysis of community structure using photographs.

The central section of each flume included a 2.4-m long sediment box that extended the width of the flume, and contained 30-cm depth of sediment. The sediment box was flanked by ~2.6 m of the fiberglass floor of the flume, along which 0.8 m was occupied by the same benthic community, but with corals and CCA resting on the bottom (i.e., “unfixed”). Members of the fixed community were buoyant weighed at the start and end of the year to measure  $G_{\text{net}}$ , but otherwise were left in place. Members of the unfixed community were removed monthly to measure buoyant weight to calculate  $G_{\text{net}}$  (described below). The unfixed portion of the community allowed monthly resolution of  $G_{\text{net}}$ , but the necessity for removal from (and return to) the flume to measure  $G_{\text{net}}$  resulted in relocation error that negated their use in photographic measurement of community structure. In addition to the coral, sand, CCA, and rubble, the flumes were augmented with holothurians (~8-cm long, *Holothuria* spp.), and macroalgae (*Turbinaria ornata* and *Halimeda minima*) to approximate the cover of these algae in the back reef in 2013 (~4–5%).

Corals, CCA, and rubble were collected from ~2-m depth in the back reef, and were attached with epoxy (Z-Spar A788) to plastic bases. Sediments were collected in the same location, and were placed into boxes that were buried in situ, flush with the sediment for 3 days to promote stratification, and then installed in each flume. Back reef communities were constructed in the flumes on 12 November 2015, and were maintained under ambient conditions until 17 November 2015, when  $p\text{CO}_2$  treatments began in three flumes, with levels increased to target values over 24 h. Throughout the experiment, the flumes were cleaned of algal turf that grew on the walls of the flumes as well as exposed plastic and the metal grid on the floor of the flume. Turfs were not removed from natural surfaces (i.e., coral bases and rubble) with the rationale that they are a normal component of back reef communities.

**Physical and chemical parameters** Seawater was circulated at ~0.1 m s<sup>-1</sup> using a pump (W. Lim Wave II 373 J s<sup>-1</sup>), and flow speeds were measured across the working sections using a Nortek Vectrino Acoustic Doppler Velocimeter. This flow speed was relevant for the back reef of Mo’orea (Hench et al. 2008). The flumes were exposed to sunlight that was shaded to a photon flux density (PFD) of photosynthetically active radiation (PAR) approximating 2-m depth in the back reef. Light was measured using cosine-corrected sensors (Odyssey, Dataflow Systems Ltd, New Zealand) that were calibrated with a LI-COR meter (LI-1400, Li-COR Biosciences, Lincoln, NE) attached to a 2 $\pi$  sensor (LI 192A). Maximum daily PFD varied by day and season

from 364 to 1831  $\mu\text{mol quanta m}^{-2} \text{s}^{-1}$ . Temperatures were regulated close to the mean monthly temperature in the back reef (Edmunds et al. 2010) that increased from ~27.8 °C in December 2015, to ~29.3 °C in April 2016, and back to ~27.4 °C in November 2016.

Seawater carbonate chemistry was uncontrolled in one flume (ambient), and in the three others, seawater pH was controlled through the addition of CO<sub>2</sub> gas (using solenoids controlled with an Aquacontroller, Neptune Systems, USA) to approximate  $p\text{CO}_2$  targets. A diurnal upward adjustment of ~0.1 pH was applied to the treatments to simulate natural variation in seawater  $p\text{CO}_2$  in the back reef (Hofmann et al. 2011). The ambient flume also maintained a diurnal variation in  $p\text{CO}_2$  with a nighttime pH ~0.1 lower than daytime. Ambient air was bubbled into all flumes.

PAR and temperature [Hobo Pro v2 ( $\pm 0.2$  °C)], Onset Computer Corp., MA, USA) were recorded, and pH was measured daily (at various times of day) on the total hydrogen ion scale (pH<sub>T</sub>). Temperature and pH were used to adjust the thermostat and pH-set points close to values that were calculated (using seacarb) to correspond to target treatments of 400  $\mu\text{atm}$ , 700  $\mu\text{atm}$ , 1000  $\mu\text{atm}$ , and 1300  $\mu\text{atm}$  (~8.04, ~7.81, ~7.70 and ~7.65, respectively). Seawater carbonate chemistry (pH and  $A_T$ ) and salinity were measured at 14:00 h and 20:00 h weekly. A conductivity meter (Thermo Scientific, Orionstar A212, Waltham, MA, USA) was used to measure salinity. The remaining parameters of the seawater carbonate system were calculated from temperature, salinity, pH<sub>T</sub>, and  $A_T$ , using the R package seacarb (Lavigne and Gattuso 2013). Calculations were made using the carbonic acid dissociation constants of Lueker et al. (2000), the  $K_{\text{SO}_4}$  concentration for the bisulfate ion from Dickson et al. (1990), and the  $K_f$  constant of Perez and Fraga (1987).

pH<sub>T</sub> was measured using a DG 115-SC electrode (Mettler Toledo, Columbus, OH, USA) that was calibrated with a TRIS buffer [SOP 6a (Dickson et al. 2007)].  $A_T$  was measured using open-cell, acidimetric titration [SOP 3b (Dickson et al. 2007)] using certified titrant with a titrator (T50 with a DG 115-SC electrode, Mettler Toledo). The accuracy and precision of measurements were determined using reference materials (from A. Dickson, Scripps Institution of Oceanography, CA, USA), against which measured values of  $A_T$  maintained an accuracy of  $1.7 \pm 0.3 \mu\text{mol kg}^{-1}$  ( $n = 15$ ) and precision of  $1.8 \pm 0.1 \mu\text{mol kg}^{-1}$  ( $n = 475$ ).

## Response variables

Net changes in mass ( $G_{\text{net}}$ ) of corals and CCA were measured using buoyant weight ( $\pm 1$  mg) (Spencer Davies 1989) by month (unfixed) or year (fixed community). Buoyant weight was converted to dry weight of CaCO<sub>3</sub> using empirical seawater density (~1.02278 g cm<sup>-3</sup>) and the density of pure aragonite (2.93 g cm<sup>-3</sup>, corals) and pure calcite

( $2.71 \text{ g cm}^{-3}$ , CCA).  $G_{\text{net}}$  in each month was expressed as the percentage change in mass relative to the initial mass in November 2015. As the area of tissue changed throughout the experiment through growth and partial mortality, “growth” could not be expressed on an area-normalized scale.

Community structure was quantified using planar photographs recorded in ambient light using a GoPro Hero 4 camera (12 MP, 3-mm focal length). The camera was moved along the flume to record the community in the working section using  $\sim 16$  frames sampling $^{-1}$ .

Photographs were analyzed using ImageJ software (Abramoff et al. 2004) (Fig. S1), in which the planar area of living tissue on corals and CCA was quantified by outlining organisms and scaling the image using the metal grid as a reference. Size ( $\text{cm}^2$ ) was expressed as a percentage of the area ( $240 \times 30 = 7200 \text{ cm}^2$ ) occupied by the fixed members of the community. The summed area of community members was used to determine overall cover of the benthic community, and changes in area were used to quantify growth. Where organisms died, their area was set to zero.

## Statistical analyses

$G_{\text{net}}$  for the unfixed community members was compared among flumes using repeated measures PERMANOVA with resemblance matrices prepared using fourth-root transformed data and Euclidian distances. Significance was evaluated in a permutational framework (999 permutations), with post hoc pair-wise contrasts between flumes conducted with *t* tests. Analyses were completed for four flumes and 9 months of data (up to and including August 2016), and for the three flumes for which a full 12 months of empirical data were available (i.e., excluding the 761  $\mu\text{atm}$  flume that malfunctioned).  $G_{\text{net}}$  for the fixed community members were compared among flumes with a Kruskal–Wallis test.

Change in area was evaluated by least squares linear regression using non-zero sizes (i.e., when the organisms were alive). Growth rates ( $\% \text{ mo}^{-1}$ ) were used to compare the responses of each taxon among flumes using Kruskal–Wallis tests with post hoc contrasts conducted with a Dwass–Steel–Critchlow–Fligner procedure. Multivariate community structure was described using non-metric multidimensional scaling (nMDS). The resemblance matrices used for nMDS cannot accommodate missing data, and missing data either were set to zero (where organisms died) or replaced by values interpolated by least squares linear regressions for each organism. Resemblance matrices were based on percent cover, and were prepared independently for each flume. Data were  $\log(x + 1)$  transformed, and converted to Bray–Curtis dissimilarities; nMDS plots were obtained using 50 iterations until stress was  $< 1.0$ . To test for differences among  $\text{pCO}_2$  treatments, resemblance matrices were

compared using rank correlation coefficients in a pairwise fashion against the resemblance matrix for the community incubated under ambient  $\text{pCO}_2$ . Similarity values were used to evaluate the extent to which communities changed over time relative to December 2015.

To evaluate the role of physical and chemical conditions (Table S1) in mediating changes in community structure, multivariate tests of association were conducted for each flume. The BEST routine in Primer 6.0 software was used to test for associations between the biological data (i.e., evaluated with Bray–Curtis dissimilarities) and the physical and chemical data (standardized values, evaluated using Euclidian Distances). Physical and chemical data (Table S1) were screened for co-linearity, and one member of each pair of co-linear variables was dropped from the analysis.

Univariate statistics were completed using Systat 13 (Systat Software Inc., San Jose, CA), and multivariate statistics were completed using Primer 6.0 (Clark and Gorley 2006).

## Results

### Overview

The physical and chemical conditions in the flumes varied (Table S1). Three  $\text{pCO}_2$  treatments were maintained for 12 months, but the 1000  $\mu\text{atm}$  flume malfunctioned after August 2016 and, therefore, was maintained for only 9 months. Mean  $\text{pCO}_2$  values differed from targets (Table S1), and hereafter are referred to as 364  $\mu\text{atm}$ , 564  $\mu\text{atm}$ , 761  $\mu\text{atm}$ , and 1067  $\mu\text{atm}$   $\text{pCO}_2$  ( $n = 12$  months for all except 761  $\mu\text{atm}$  where  $n = 9$  months).

Temperature and PFD differed seasonally, but were similar among flumes. The mean maximum daytime PFD on the days of measurement across the whole year varied between  $974 \pm 159 \mu\text{mol quanta m}^{-2} \text{ s}^{-1}$  (364  $\mu\text{atm}$  treatment) and  $1196 \pm 142 \mu\text{mol quanta m}^{-2} \text{ s}^{-1}$  (564  $\mu\text{atm}$  treatment), and mean monthly temperatures across the whole year varied between  $28.0 \pm 0.4 \text{ }^\circ\text{C}$  (400  $\mu\text{atm}$  treatment) and  $28.1 \pm 0.3 \text{ }^\circ\text{C}$  (1000  $\mu\text{atm}$  treatment) (all  $\pm$  SE,  $n = 12$  months, except for the 761  $\mu\text{atm}$  flume where  $n = 9$ ) (Table S1). Seasonal effects were strong, with mean monthly temperatures varying from a summer high of  $29.3 \pm 0.1 \text{ }^\circ\text{C}$  (April, 2016) to a winter low of  $25.8 \pm 0.2 \text{ }^\circ\text{C}$  (September 2016), and mean monthly PFD (averaged across all records and days in each month) varying from an autumn low of  $129 \pm 15 \mu\text{mol quanta m}^{-2} \text{ s}^{-1}$  (February 2016) to a spring high of  $518 \pm 9 \mu\text{mol quanta m}^{-2} \text{ s}^{-1}$  (November 2016) (all  $\pm$  SD,  $n = 4$  flumes). Seasonal effects were accompanied by warming (mostly December 2015 to March 2016) and cooling (mostly July 2016 to September 2016), and months in which PAR was decreasing (Table S1) (December 2015,



January, April and October 2016), or increasing (February, March, May–September, and November 2016).

Following establishment of the communities on 12 November 2015, a few organisms died in the first 2 weeks and were replaced. Organisms were not replaced after the first month, although a small number of organisms continued to die, with these scattered among all flumes.

When the pictures were recorded on 15 December 2015 (Fig. S1), the flumes contained 2–6 colonies of *Porites rus* (mean areas of 68–108 cm<sup>2</sup>), 9–10 massive *Porites* (68–119 cm<sup>2</sup>), 4 *Montipora* (70–73 cm<sup>2</sup>), 2–3 *P. verrucosa* (52–162 cm<sup>2</sup>), 2 pieces of *Lithophyllum kotschyianum* (53–83 cm<sup>2</sup>), and 5–6 *P. onkodes* (40–70 cm<sup>2</sup>). At this time, coral cover in the central portion of the flumes was 25% in the 364 µatm flume, 27% in the 564 µatm flume, and 27% in the 761 µatm flume. Coral cover in the central portion of the 1067 µatm flume was 18%, and departure from the ~25% in the other flumes was caused by placing larger numbers of corals in unfixed portions of flume. Coral cover in the 5-m working section of the 1067 µatm flume was 24% (15 November 2015).

Most corals and *Lithophyllum kotschyianum* survived, although *P. onkodes* died, and one coral split into two. The 761 µatm pCO<sub>2</sub> flume malfunctioned after 15 August 2016, and results for this flume were truncated. Biological responses in this flume were interpolated for September–November and used in the multivariate analysis as described below.

### Variation in G<sub>net</sub>

Of the four coral species and two CCA species incubated in the flumes, there were sufficient replicates (i.e., ≥4 colonies) of massive *Porites*, *Montipora*, and *P. onkodes* for analysis of G<sub>net</sub>. In November 2015 in the unfixed community, the mean mass (±SE) of massive *Porites* ranged from 199 ± 26 g (761 µatm flume) to 265 ± 56 g (1300 µatm), for *Montipora* it varied from 101 ± 25 g (1300 µatm flume) to 184 ± 50 g (564 µatm flume), and for *P. onkodes* it varied from 77 ± 13 g (364 µatm flume) to 147 ± 51 g (564 µatm flume). For the three treatments that operated over a year, two coral colonies declined in mass (one massive *Porites* in the 1067 µatm flume, and one *Montipora* in the 364 µatm flume). Virtually all (94%) of the *P. onkodes* declined in mass in the three flumes that operated for a year. Similar trends for changes in organism mass were observed in the 761 µatm flume, which operated until August 2015. For the unfixed community, G<sub>net</sub> of massive *Porites*, *Montipora* and *P. onkodes* differed among four flumes over 1 year (Pseudo- $F \geq 3.63$   $df = 3147-547$ ,  $P_{\text{perm}} \leq 0.006$ ) and also among three flumes over 9 months (Pseudo- $F \geq 26.49$ ,  $df = 3141-531$ ,  $P_{\text{perm}} = 0.001$ ) (Fig. 1). Over 9 months and for massive *Porites*, G<sub>net</sub> was reduced, but still positive, at 1067 µatm

and 564 µatm relative to ambient ( $P_{\text{perm}} \leq 0.050$ ), but was not different between 761 µatm and ambient ( $P_{\text{perm}} = 0.524$ ); for *Montipora*, G<sub>net</sub> was reduced, but still positive, at 762 and 1067 µatm versus ambient ( $P_{\text{perm}} \leq 0.004$ ), but was not different between 761 µatm and ambient ( $P_{\text{perm}} = 0.096$ ); and for *P. onkodes*, G<sub>net</sub> was reduced and negative at high pCO<sub>2</sub> relative to ambient ( $P_{\text{perm}} \leq 0.003$ ). Relative differences in G<sub>net</sub> were similar for the three flumes that were incubated over 12 months, except G<sub>net</sub> for massive *Porites* did not differ between 564 µatm and ambient ( $P_{\text{perm}} = 0.846$ ) (Fig. 1). Median relative G<sub>net</sub> in November 2016 declined from 122% at ambient to 108% at 1067 µatm for massive *Porites*, from 144 to 124% for *Montipora*, and from 100 to 93% for *P. onkodes*.

For the members of the fixed community, G<sub>net</sub> responded differently to the treatments compared to the unfixed community (Fig. 1), and was unaffected by treatments for massive *Porites* and *Montipora* ( $H \leq 1.086$ ,  $P \geq 0.581$ ). For *P. onkodes*, G<sub>net</sub> differed among treatments ( $H = 6.009$ ,  $n_1, n_2, n_3 = 6$ ,  $P = 0.049$ ), and was reduced at high pCO<sub>2</sub> ( $P = 0.006$ ).

### Hypothesis 1: effects of pCO<sub>2</sub> on planar growth

For the corals and one alga analyzed for size (Fig. S2), in a few cases it was not possible to measure planar area. In these cases, the distorted image was discarded, and the missing area replaced with a value interpolated using a linear regression of size ( $n = 8-11$  records) against time (Fig. 2, Table S2). Overall, the growth rates of most corals were reduced with increases in pCO<sub>2</sub>, and the growth rates of the alga *Lithophyllum kotschyianum* largely were unaffected (Table S2).

Growth rates (Fig. 2) did not differ among flumes for *Montipora* ( $H = 1.103$ ,  $n_1 = n_2 = n_3 = n_4 = 4$ ,  $P = 0.776$ ), *P. rus* ( $H = 6.611$ ,  $n_1 = 2$ ,  $n_2 = 6$ ,  $n_3 = 6$ ,  $n_4 = 4$ ,  $P = 0.085$ ), *P. verrucosa* ( $H = 3.418$ ,  $n_1 = 2$ ,  $n_2 = 3$ ,  $n_3 = 2$ ,  $n_4 = 3$ ,  $P = 0.332$ ), or *Lithophyllum kotschyianum* ( $H = 0.667$ ,  $n_1-n_4 = 2$ ,  $P = 0.881$ ). Growth rates differed among flumes for massive *Porites* ( $H = 8.009$ ,  $n_1 = 9$ ,  $n_2 = 8$ ,  $n_3 = 9$ ,  $n_4 = 11$ ,  $P = 0.046$ ), with post hoc analyses revealing this reflected higher growth rates at 364 µatm versus 564 µatm ( $W = 5.443$ ,  $P = 0.001$ ), and a trend for higher growth rates at 364 µatm versus 1067 µatm ( $W = 3.559$ ,  $P = 0.057$ ); no other contrasts differed ( $P \geq 0.449$ ).

### Hypothesis 2: effects of pCO<sub>2</sub> on community structure

Multivariate analyses were conducted with nMDS using the percentage cover of organisms in which missing values were replaced by: (a) values interpolated using the linear regressions of size on time (Table S2), or (b) when these values were negative or the organisms died (notably in the 761

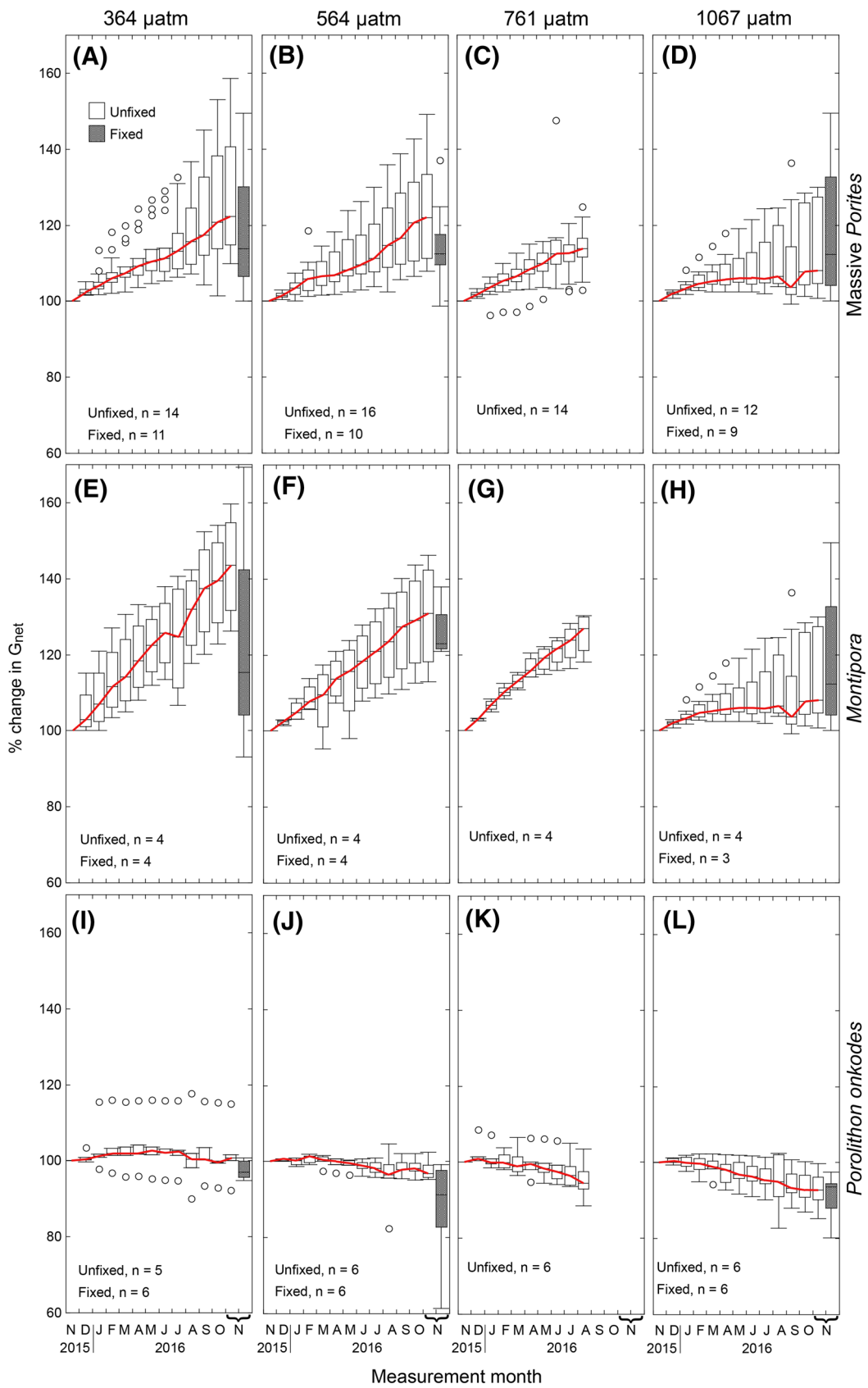


**Fig. 1** Box plots showing  $G_{\text{net}}$  of corals and algae relative to their weight at the start of the experiment for the four treatments, 364  $\mu\text{atm}$  (ambient), 564  $\mu\text{atm}$ , 761  $\mu\text{atm}$ , and 1067  $\mu\text{atm}$   $p\text{CO}_2$ . The 761  $\mu\text{atm}$  flume malfunctioned after August and buoyant weights were not recorded thereafter. Box plots display medians as a line within each box (linked by red lines for the unfixed community), boxes show the quartiles, and whiskers display  $\times 1.5$  the interquartile range, with outliers plotted individually. Sample sizes are shown in each plot frame for unfixed and fixed organisms

$\mu\text{atm}$  flume after August 2016), with zero. This procedure resulted in 12% interpolated values in the 364  $\mu\text{atm}$  flume ( $n=264$  records), 10% interpolated values in the 564  $\mu\text{atm}$  flume ( $n=264$  records), 38% interpolated values in the 761  $\mu\text{atm}$  flume ( $n=286$  records, with all values for September, October, and November interpolated due to equipment malfunction), and 11% interpolated values in the 1067  $\mu\text{atm}$  flume ( $n=220$  records).

nMDS separated communities among months (Fig. 3). Communities changed from summer to spring, and the changes under the three elevated  $p\text{CO}_2$  treatments differed from ambient conditions (364  $\mu\text{atm}$ ). In ambient conditions, the community changed from December 2015 to October 2016, but changes accelerated with the onset of spring until November 2016. In contrast, the communities under elevated  $p\text{CO}_2$  changed between December 2015 and January 2016, but did not show a spring acceleration of change. The causes of the changes in overall community structure are revealed by the vectors displaying associations between organism size and the nMDS axes. Variation in abundances of all taxa (increases and decreases) were responsible for the changes in community structure under 364  $\mu\text{atm}$  (i.e., ambient), with a decline in sizes of *P. rus*, massive *Porites*, and *Montipora* changing community structure between December 2015 and January 2016 (Fig. 3a). Under elevated  $p\text{CO}_2$ , the changes in community structure were driven by declining sizes of massive *Porites* and increasing sizes of *Montipora* and *P. verrucosa*. The change in community structure that occurred in the spring under ambient  $p\text{CO}_2$  was associated with rapid growth by *P. verrucosa* and massive *Porites*, and shrinkage of *Montipora*, and was almost fully attenuated at high  $p\text{CO}_2$ .

Based on a priori Spearman rank correlations to compare resemblance matrices of treatments against ambient  $p\text{CO}_2$ , the change in community structure in the 364  $\mu\text{atm}$  flume differed from that observed in the 564  $\mu\text{atm}$  flume ( $\rho=0.526$ ,  $P_{\text{perm}}=0.009$ ), the 761  $\mu\text{atm}$  flume ( $\rho=0.721$ ,  $P_{\text{perm}}=0.001$ ), and the 1067  $\mu\text{atm}$  flume ( $\rho=0.716$ ,  $P_{\text{perm}}=0.001$ ). As the incubations lengthened, communities differed more from their initial state (Fig. S3). In the summer, autumn, and winter, the community in the 1067  $\mu\text{atm}$  flume was more similar to the community in December 2015 than was the case with the communities in the 564  $\mu\text{atm}$  and 761  $\mu\text{atm}$  flumes (Fig. S3a-c). With the onset of spring, the community in the ambient flume underwent a rapid divergence from the

community structure recorded in December 2015, but this effect was attenuated in the 564  $\mu\text{atm}$  and 1067  $\mu\text{atm}$  flumes (Fig. S3D). This analysis suggests that the community in the 761  $\mu\text{atm}$  flume diverged from the December 2015 structure in the spring.

### Hypothesis 3: association of community structure with treatment conditions

The physical and chemical conditions (Table S1) were evaluated for their capacity to explain variation in the biotic data using a Spearman rank correlations after screening standardized abiotic data for co-linearity. Based on this screening, the analysis employed mean monthly seawater temperature (MMT), the slope of mean daily seawater temperature over time (days) over the month prior to sampling (SMDT),  $p\text{CO}_2$ , the light integrated over the day of sampling (ILI), mean PFD over the day of sampling (MeLIM), and the slope of PFD integrated by day on time (days) over the month prior to sampling (SILI), as predictor variables (Table S1). For the 564  $\mu\text{atm}$  flume, the change in community structure was best explained by MMT and SILI ( $P_{\text{perm}} < 0.010$ ) and no other combination of variables was significant ( $P_{\text{perm}} \geq 0.050$ ). Variation in community structure in the ambient flume (364  $\mu\text{atm}$ ), the 761  $\mu\text{atm}$  flume (December 2015–August 2016 only), and the 1067  $\mu\text{atm}$  flume, were not explained by any combination of abiotic drivers ( $P_{\text{perm}} \geq 0.209$ ) (Table 1).

## Discussion

In the present study, high  $p\text{CO}_2$  affected back reef communities to cause declines in  $G_{\text{net}}$ , with small effects on organism size, and subtle effects on community structure. These results suggest that the cover of reef communities may be more resistant to OA than is the net calcification of the corals and calcified algae responsible for producing the reef framework.

Relative to previous studies of OA on coral reefs (Chan and Connolly 2012), our analysis of  $G_{\text{net}}$  is most similar to the response of “growth” or “calcification” that are reported in other studies. Although the challenges of long-duration experiments precluded the use of “growth” in the present study,  $G_{\text{net}}$  provides an ecologically relevant measure of the effects of OA on carbonate skeletons (Silverman et al. 2007) that integrates calcification, dissolution, and accretion by taxa other than the focal organisms (i.e., the corals and calcified algae). While these effects cannot be distinguished in the present study, nevertheless the outcome is important in corroborating the threat posed to carbonate reef frameworks by high  $p\text{CO}_2$  in seawater (Silverman et al. 2007). Interestingly, variation in  $G_{\text{net}}$  by taxon (and relative to the initial mass) as the experiment progressed generally increased for both the

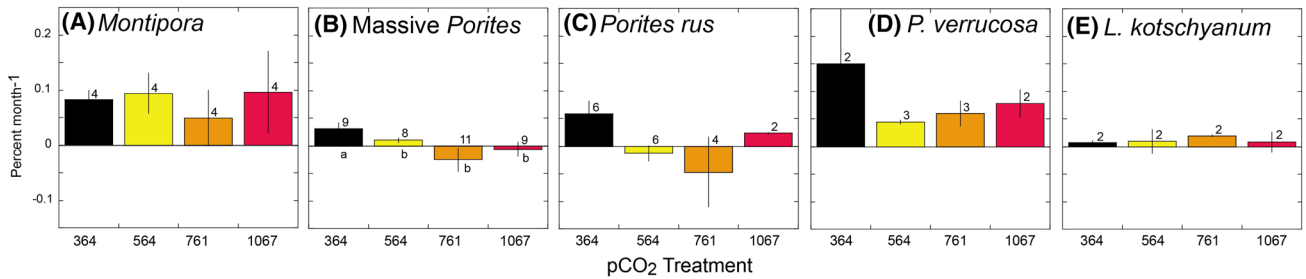


**Fig. 2** Mean ( $\pm$ SE) growth (i.e., change in cover over time) of corals and algae (as in Fig. S2) in flumes incubated in each pCO<sub>2</sub> treatment. Changes in cover are calculated as least squares slopes of planar area on time in cases with  $\geq 4$  records (shorter records were excluded),

and not all slopes were statistically significant (ESM). Growth rates differed among treatments for massive *Porites* (but not for any other taxa), and significant differences from post hoc contrasts are shown by dissimilar letters. Sample sizes are shown above each bar

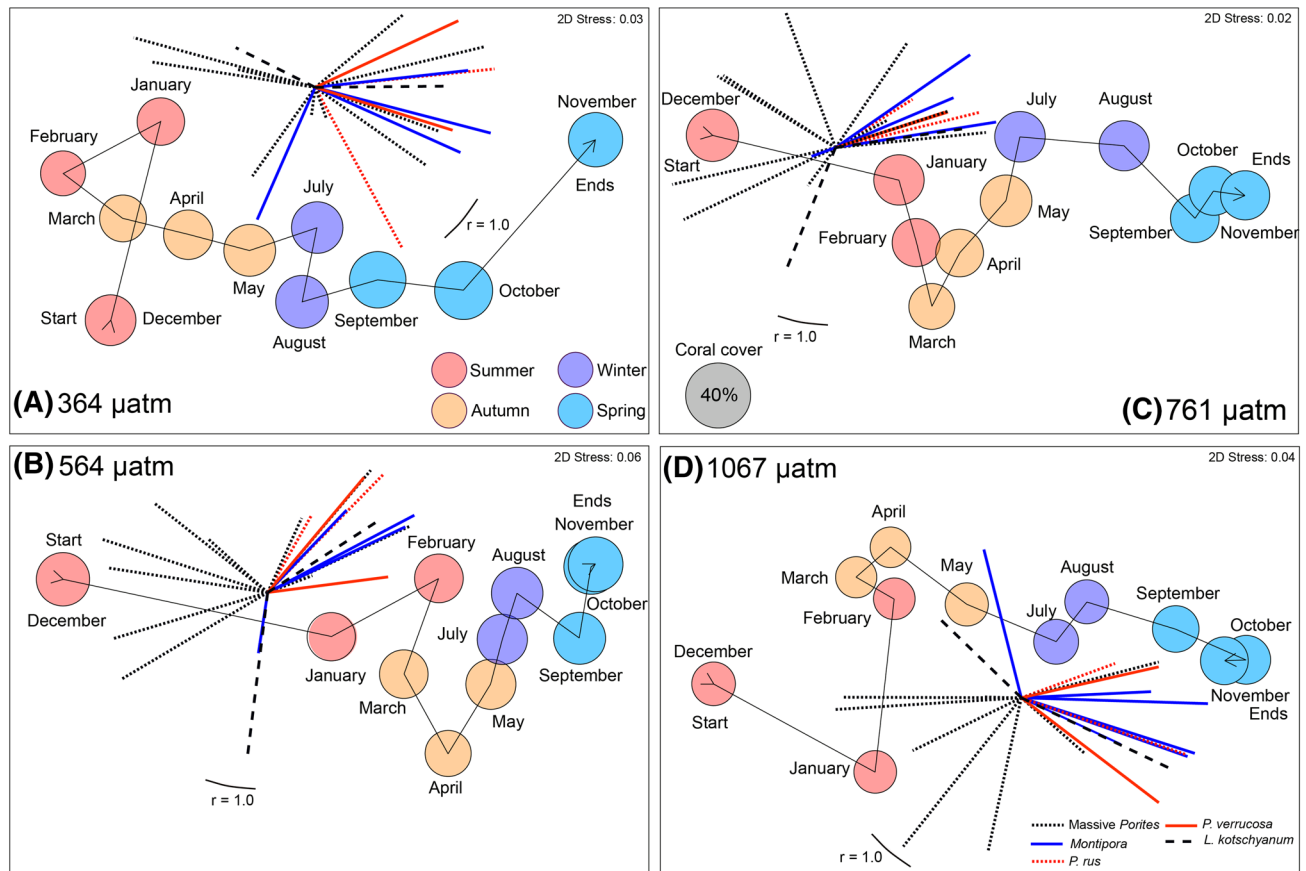


**Fig. 3** nMDS coral reef community structure (Fig. S1) in flumes incubated under each pCO<sub>2</sub> treatment. Circles are scaled to coral cover and colored by season (legend in a), and are sequentially linked by a vector. Overlaid vector plots display Pearson correlations (scaled

to  $r=1.0$ ) of size of each replicate organism on each nMDS axis (legend in d) and, therefore, each taxon is displayed as multiple vectors. Vector plots reveal the influence of each organism in separating communities in two-dimensional space along the X and Y axes

unfixed and fixed members of the community, suggesting that replicates of each taxon diverged in performance from another as time progressed. These effects probably reflect within-species genetic variation in the susceptibility to OA (Shaw et al. 2016). Despite the responses of  $G_{net}$  to OA in the present study, the analyses of community structure do

not reveal strong effects of OA, suggesting that this emergent property may be resilient to OA on a time scale of 1 year. While preliminary work conducted prior to the main experiment, as well as the ultimate effects of OA on growth (e.g., for massive *Porites*) and community structure, suggest treatment effects were not constrained by Type II error, it is not



**Table 1** Summary of multivariate analyses testing for the capacity of abiotic data to explain biotic data in a Spearman rank correlation analysis ( $\rho$ ) analyzed within a permutation framework ( $P_{\text{perm}}$ )

Biotic data	IV	$\rho$	$P_{\text{perm}}$
Flume 3—364 $\mu\text{atm}$	n/a	0.141	0.209
Flume 2—564 $\mu\text{atm}$	MMT, SILI	0.604	< 0.010
Flume 4—761 $\mu\text{atm}$	n/a	0.479	0.379
Flume 1—1067 $\mu\text{atm}$	n/a	0.293	0.446

Abiotic data were selected after screening for co-linearity, and included six independent variables (IV): MMT, SMDT,  $\text{pCO}_2$ , ILI, MeLIM, and SILI (Table S1). Analysis for the 761  $\mu\text{atm}$  considered December 2015 to August 2016 as this flume malfunctioned after this sampling

possible to exclude statistical power as one factor limiting the detection of stronger effects on community structure.

### Hypothesis 1: effects of $\text{pCO}_2$ on planar growth

Our analyses revealed changes in organism size as a function of  $\text{pCO}_2$ , and these were significant for massive *Porites*. For this taxon, mean growth rates were depressed by 68% at 564  $\mu\text{atm}$   $\text{pCO}_2$  compared to ambient conditions. In terms of planar growth, our results for four of five taxa appear inconsistent with the generalized findings that the calcification of corals and CCA is depressed by high  $\text{pCO}_2$  (Kuffner et al. 2008; Kroeker et al. 2013), and with previously reported declines in mass deposition of  $\text{CaCO}_3$  at high  $\text{pCO}_2$  for massive *Porites*, *Porites rus*, *P. verrucosa* and *L. kotschyianum* in Mo'orea (Comeau et al. 2014).

Critical considerations in the comparison of the present patterns with previous findings include: (a) the analysis here of planar area, and (b) the negative effect of OA on  $G_{\text{net}}$ . Such comparisons also emphasize the gap between studies of OA on coral reefs (Chan and Connolly 2012) and ecological analyses of coral reef communities. Bridging this gap was an important objective of the present study, and while we have made progress towards this outcome, it is clear that this objective is complex and will require further research to fully achieve. A limitation of the approach employed herein is the use of least squares slopes of percentage cover on time to estimate growth, where many slopes (57% pooled among flumes and taxa, 25–87% by taxon, pooled among flumes) were not statistically significant as a result of low sample sizes ( $n=8$ –11 months), slopes that approached zero (e.g., *L. kotschyianum*), or variable organism sizes attributed to parallax (e.g., *P. verrucosa*). Rather than setting non-significant slopes to zero, which creates values of unknown distribution that are likely to be biased, we used least squares estimates of slopes to estimate the relationships between area and time. Limitations of this assumption are revealed by the error bars associated with the mean growth rates (Fig. 2).

An expectation of comparable effects of  $\text{pCO}_2$  on mass accretion and linear extension (and change in planar area) for calcifiers assumes a fixed relationship between these measures of growth, which would reflect constant skeletal density and uniform deposition of  $\text{CaCO}_3$  across the skeleton surface. Both assumptions are incorrect, as coral skeletons vary in density and  $\text{CaCO}_3$  is deposited heterogeneously across their surface (Pratchett et al. 2015). These aspects of coral biology recently have been discovered by the OA research community, which has reported that the effects of OA on *Porites* are modulated by skeleton density and focal deposition of  $\text{CaCO}_3$  (Mollica et al. 2018). Moreover, as studies of the effects of OA on coral reefs have extended to communities (Dove et al. 2013), it has become clear that much of the OA-mediated decline in net community calcification is attributed to dissolution (Andersson 2015; Comeau et al. 2015, 2016), which is independent of the sizes of coral colonies and their growth rates. Together, the aforementioned effects provide an explanation for our results, because they can reconcile depressed net calcification under OA (Chan and Connolly 2012; Comeau et al. 2015, 2016), with limited effects on community structure.

### Hypothesis 2: effects of $\text{pCO}_2$ on community structure

Given the longevity of our experiment, its ecological relevance, and the negative effects of high  $\text{pCO}_2$  on  $G_{\text{net}}$  [as expected (Chan and Connolly 2012; Comeau et al. 2015, 2016)], it is striking that the effects of the treatments on community structure were modest. The cover of most taxa varied over time and changed multivariate community structure in dissimilar ways in the  $\text{pCO}_2$  treatments versus ambient conditions. However, these effects were subtle and statistically were explained weakly by  $\text{pCO}_2$ , and more strongly by irradiance and temperature. In contrast to the hardiness of massive *Porites* to elevated  $\text{pCO}_2$  (Comeau et al. 2016), and its abundance at naturally elevated  $\text{pCO}_2$  sites (Fabricius et al. 2011; Barkley et al. 2015), a decline in relative abundance of this taxon in our flumes was one of the distinctive trends associated with high  $\text{pCO}_2$ .

There are few studies with which the present analysis can be compared, but one is provided by an experiment in which reef communities were incubated under OA conditions for ~84 days (Dove et al. 2013). This experiment tested the responses of communities in 300-L tanks to preindustrial, present, and future conditions arising from anthropogenic  $\text{CO}_2$  emissions, and contrasted 301  $\mu\text{atm}$   $\text{pCO}_2/25.2$  °C, 405  $\mu\text{atm}/26.1$  °C, 611  $\mu\text{atm}/28.5$  °C, and 1009  $\mu\text{atm}/30.2$  °C. These treatments differ from those employed in the present study, as we did not manipulate temperature, but three of the treatments are close to our 364  $\mu\text{atm}/28.0$  °C, 761  $\mu\text{atm}/27.5$  °C, and 1067  $\mu\text{atm}/28.0$  °C flumes. Dove et al.

(2013) began their experiment with 35% coral cover (eight genera) and 15% macroalgae (including CCA), but four coral genera bleached and died at 611  $\mu\text{atm}/28.5\text{ }^\circ\text{C}$  and 1009  $\mu\text{atm}/30.2\text{ }^\circ\text{C}$ . While Dove et al. (2013) did not distinguish among taxa, they found that net calcification was depressed at 611  $\mu\text{atm}/28.5\text{ }^\circ\text{C}$  and 1009  $\mu\text{atm}/30.2\text{ }^\circ\text{C}$  relative to 405  $\mu\text{atm}/26.1\text{ }^\circ\text{C}$  (by 78–87% for buoyant weight of coral colonies, and 52–138% for daily community metabolism), yet coral cover declined 29–31%, with a 9% decline in the controls. While the relative roles of  $\text{pCO}_2$  and temperature in driving these trends cannot be separated, they underscore a similar outcome to that observed in the present study.

Over times scales of decades–centuries, there is evidence of strong effects of high seawater  $\text{pCO}_2$  on coral community structure. This evidence comes from coral reefs adjacent to volcanic  $\text{CO}_2$  seeps (Fabricius et al. 2011), or growing across a gradient of  $\text{pCO}_2$  (Barkley et al. 2015). On coral reefs fringing the D'Entrecasteaux Islands (Papua New Guinea),  $\text{CO}_2$  seeps create a gradient of seawater  $\text{pCO}_2$  from 296 to 953  $\mu\text{atm}$  (at median temperatures of 27.7–29.0  $^\circ\text{C}$ ), across which coral cover remains  $\sim 32\%$ , and the calcification of massive *Porites* is unchanged (Fabricius et al. 2011). However, coral reef community structure differs across the gradient, with high  $\text{pCO}_2$  associated with a greater cover of massive *Porites*, lower coral richness, reduced densities of juvenile corals, and lowered abundance of calcified red algae (Fabricius et al. 2011). In contrast, in the Palau Rock Islands, 11 sites provide a contrast of seawater  $\text{pCO}_2$  from 370 to 604  $\mu\text{atm}$ , and across this gradient, there is no change in cover of coral, macroalgae, CCA, or the richness and diversity of coral genera, yet community structure differs (Barkley et al. 2015). The calcification and linear extension of massive *Porites* and *Favia* does not vary over the gradient, although massive *Porites* is more extensively bioeroded at high  $\text{pCO}_2$  sites (Barkley et al. 2015).

Taken together, the present analysis, one comparable study (Dove et al. 2013), and analyses of coral reefs in locations with naturally high  $\text{pCO}_2$ , underscore: (a) the weak relationship between net calcification and community structure at high  $\text{pCO}_2$ , (b) the potential for reef communities to adjust through changes in composition and abundances to maintain benthic cover (at coarse resolution), and (c) the potential fragility of these altered states due to depressed  $G_{\text{net}}$  (and enhanced dissolution) of the framework upon which they are built (Comeau et al. 2016).

### Hypothesis 3: association of community structure with treatment conditions

While coral reef community structure changed over time, as expected from differential growth of the replicates of each taxon, and differed among treatments, variation was only weakly associated with physical and chemical

conditions. In the relationships examined for the four flumes, 6 of 12 variables—mean monthly temperature (MMT), the slope of daily temperature against time (SMDT),  $\text{pCO}_2$ , daily integrated PFD (ILI), mean PFD over the month prior to sampling (MeLIM), and the slope of daily integrated PFD on time for the month prior to sampling (SILI)—were only significant for the 564  $\mu\text{atm}$  flume, where combinations of light and temperature (SILI and MMT) had value in explaining variation in community structure.  $\text{pCO}_2$  (which was collinear with pH) had no statistically discernable effect in changing community structure. This outcome does not mean that community structure was unaffected by OA, rather that the effects were small relative to the capacity of the community to “adjust” to a diversity of conditions that varied naturally during the year.

Overall, the weak associations between community structure and these potential environmental drivers reflect three effects. First, the relative changes in community structure were small and, therefore, there was little variation to statistically explain (i.e., the “effect-size” hypothesis). Second, the community responded to environmental drivers through multiple biological processes, and therefore, numerous pathways of causation contributed to the challenges of detection (i.e., the “diverse-driver” hypothesis). Third, and of greatest relevance to understanding the response of coral reefs to OA, is the likelihood that the community is “adjusting” to the environmental conditions to create community stability (the “adjustment hypothesis”).

## Summary

To our knowledge, this study is one of the longest experimental analysis of the effects of OA on coral reefs. While revealing inhibitory effects of OA on  $G_{\text{net}}$ , our results suggest that back reef communities are able to minimize observable changes in community structure. These changes were small even though net community calcification was impaired by elevated  $\text{pCO}_2$  (Carpenter et al. 2018) and, therefore, the potential for an unobservable, but weakened (i.e., less dense) framework was created for the coral reef community. Over  $> 1$  year, it is unknown how long such mechanisms could prevent profound changes from occurring in coral reef community structure (sensu Hoegh-Guldberg et al. 2007) as a result of OA.

**Acknowledgements** We thank the staff of the Richard B. Gump South Pacific Research Station for supporting our research. Research was completed under permits issued by the Haut-commissariat de la République en Polynésie Française (DRRT) (Protocole d'Accueil 2015–2016). This is contribution number 287 of the CSUN Marine Biology Program.

**Funding** Funding was provided by the National Science Foundation grants (OCE 14-15268, and 12-36905). All applicable international, national, and/or institutional guidelines for the care and use of animals were followed. Research was completed under permits issued by the Haut-commissariat de la République en Polynésie Française (DRRT) (Protocole d'Accueil 2015–2016).

## Compliance with ethical standards

**Conflict of interest** The authors have no conflict of interests.

**Data accessibility** The data for this project are hosted at <http://mcr.lternet.edu> and can be accessed using doi:<https://doi.org/10.6073/pasta/6aae5ade59fb1a912f659c1336e34091>.

## References

- Abramoff MD, Magalhães P, Ram SJ (2004) Image processing with ImageJ. *Biophotonics Int* 11:36–43
- Albright R, Takeshita Y, Koweek DA, Ninokawa A, Wolfe K, Rivlin T, Nebuchina Y, Young J, Caldeira K (2018) Carbon dioxide addition to coral reef waters suppresses net community calcification. *Nature* 555:516–519. <https://doi.org/10.1038/nature25968>
- Andersson AJ (2015) A fundamental paradigm for coral reef carbonate sediment dissolution. *Front Mar Sci*. <https://doi.org/10.3389/fmars.2015.00052>
- Barkley HC, Cohen AL, Golbuu Y, Starczak VR, DeCarlo TM, Shamberger KEF (2015) Changes in coral reef communities across a natural gradient in seawater pH. *Sci Adv*. <https://doi.org/10.1126/sciadv.1500328>
- Carpenter RC, Lantz CA, Shaw E, Edmunds PJ (2018) Responses of coral reef community metabolism in flumes to ocean acidification. *Mar Biol*. <https://doi.org/10.1007/s00227-018-3324-0>
- Chan NCS, Connolly SR (2012) Sensitivity of coral calcification to ocean acidification: a meta-analysis. *Glob Change Biol* 19:282–290. <https://doi.org/10.1111/gcb.12011>
- Clark KR, Gorley RN (2006) PRIMER V6: User Manual/tutorial. PRIMER-E, Plymouth
- Comeau S, Edmunds PJ, Spindel NB, Carpenter RC (2014) Fast coral reef calcifiers are more sensitive to ocean acidification in short-term laboratory incubations. *Limnol Oceanogr* 59:1081–1091. <https://doi.org/10.4319/lo.2014.59.3.1081>
- Comeau S, Carpenter RC, Lantz CA, Edmunds PJ (2015) Ocean acidification accelerates dissolution of experimental coral reef communities. *Biogeosciences* 12:365–372. <https://doi.org/10.5194/bg-12-365-2015>
- Comeau S, Lantz CA, Edmunds PJ, Carpenter RC (2016) Framework of barrier reefs threatened by ocean acidification. *Glob Change Biol* 22:1225–1234. <https://doi.org/10.1111/gcb.13023>
- Dickson AG, Wesolowski DJ, Palmer DA, Mesmer RE (1990) Dissociation constant of bisulfate ion in aqueous sodium chloride solutions to 250 °C. *J Phys Chem* 94:7978–7985. <https://doi.org/10.1021/j100383a042>
- Dickson AG, Sabine CL, Christian JR (eds) (2007) Guide to best practices for ocean CO<sub>2</sub> measurements. North Pacific Marine Science Organization, Sidney
- Dove SG, Kline DI, Pantos O, Angly FE, Tyson GW, Hoegh-Guldberg O (2013) Future reef decalcification under a business-as-usual CO<sub>2</sub> emission scenario. *Proc Natl Acad Sci USA* 110:15342–15347. <https://doi.org/10.1073/pnas.1302701110>
- Edmunds PJ (2015) MCR LTER: coral reef: long-term population and community dynamics: corals, ongoing since 2005 environmental data initiative. <https://doi.org/10.6073/pasta/1f05f1f52a2759dc096da9c24e88b1e8>
- Edmunds P, Leichter J, Adjeroud M (2010) Landscape-scale variation in coral recruitment in Moorea, French Polynesia. *Mar Ecol Prog Ser* 414:75–89. <https://doi.org/10.3354/meps08728>
- Fabricius KE, Langdon C, Uthicke S, Humphrey C, Noonan S, De'ath G, Okazaki RR, Muehllehner N, Glas MS, Lough JM (2011) Losers and winners in coral reefs acclimatized to elevated carbon dioxide concentrations. *Nat Clim Change* 1:165–169. <https://doi.org/10.1038/nclimate1122>
- Fabricius KE, De'ath G, Noonan S, Uthicke S (2014) Ecological effects of ocean acidification and habitat complexity on reef-associated macroinvertebrate communities. *Proc R Soc B*. <https://doi.org/10.1098/rspb.2013.2479>
- Hench JL, Leichter JJ, Monismith SG (2008) Episodic circulation and exchange in a wave-driven coral reef and lagoon system. *Limnol Oceanogr* 53:2681–2694. <https://doi.org/10.4319/lo.2008.53.6.2681>
- Hoegh-Guldberg O, Mumby PJ, Hooten AJ, Steneck RS, Greenfield P, Gomez E, Harvell CD, Sale PF, Edwards AJ, Caldeira K et al (2007) Coral reefs under rapid climate change and ocean acidification. *Science* 318:1737–1742. <https://doi.org/10.1126/science.1152509>
- Hofmann GE, Smith JE, Johnson KS, Send U, Levin LA, Micheli F, Paytan A, Price NN, Peterson B, Takeshita Y et al (2011) High-frequency dynamics of ocean pH: a multi-ecosystem comparison. *PLoS One*. <https://doi.org/10.1371/journal.pone.0028983>
- IPCC (2014) Climate change 2014: synthesis report. In: Core Writing Team, Pachauri RK, Meyer LA (eds) Contribution of working groups I, II and III to the fifth assessment report of the intergovernmental panel on climate change. IPCC, Geneva
- Kornder NA, Riegl BM, Figueredo J (2018) Thresholds and drivers of coral calcification responses to climate change. *Glob Change Biol* 24:5084–5095
- Kroeker KJ, Kordas RL, Crim RN, Singh GG (2010) Meta-analysis reveals negative yet variable effects of ocean acidification on marine organisms. *Ecol Lett* 13:1419–1434. <https://doi.org/10.1111/j.1461-0248.2010.01518.x>
- Kroeker KJ, Kordas RL, Crim R, Hendriks IE, Ramajo L, Singh GS, Duarte CM, Gattuso JP (2013) Impacts of ocean acidification on marine organisms: quantifying sensitivities and interaction with warming. *Glob Change Biol* 19:1884–1896. <https://doi.org/10.1111/gcb.12179>
- Kuffner IB, Andersson AJ, Jokiel PL, Rodgers KS, Mackenzie FT (2008) Decreased abundance of crustose coralline algae due to ocean acidification. *Nat Geosci* 1:114–117. <https://doi.org/10.1038/ngeo100>
- Langdon C, Takahashi T, Sweeney C, Chipman D, Goddard J, Marubini F, Aceves H, Barnett H, Atkinson MJ (2000) Effect of calcium carbonate saturation state on the calcification rate of an experimental coral reef. *Glob Biogeochem Cycles* 14:639–654. <https://doi.org/10.1029/1999GB001195>
- Lavigne H, Gattuso JP (2013) Seacarb, seawater carbonate chemistry with R. R package version 2.4.10. <https://CRAN.R-project.org/package=seacarb>. Accessed 11 July 2014
- Lueker TJ, Dickson AG, Keeling CD (2000) Ocean pCO<sub>2</sub> calculated from dissolved inorganic carbon, alkalinity, and equations for K-1 and K-2: validation based on laboratory measurements of CO<sub>2</sub> in gas and seawater at equilibrium. *Mar Chem* 70:105–119
- Mollica NR, Guo W, Cohen AL, Huang K-F, Foster GL, Donald HK, Solow AR (2018) Ocean acidification affects coral growth by reducing skeletal density. *Proc Natl Acad Sci USA* 115:1754–1759. <https://doi.org/10.1073/pnas.1712806115>
- Perez FF, Fraga F (1987) Association constant of fluoride and hydrogen ions in seawater. *Mar Chem* 21:161–168

- Pratchett MS, Anderson KD, Hoogenboom MO, Widman E, Baird AH, Pandolfi JM, Edmunds PJ, Lough JM (2015) Spatial, temporal and taxonomic variation coral growth—implications for the structure and function of coral reef ecosystems. In: Hughes RN, Hughes DJ, Smith IP, Dale AC (eds) *Oceanography and marine biology: an annual review*. CRC Press, Boca Raton, pp 215–295
- Shaw EC, Carpenter RC, Lantz CA, Edmunds PJ (2016) Intraspecific variability in the response to ocean warming and acidification in the scleractinian coral *Acropora pulchra*. *Mar Biol* 163:210. <https://doi.org/10.1007/s00227-016-2986-8>
- Silverman J, Lazar B, Erez J (2007) Effects of aragonite saturation, temperature, and nutrients on the community calcification rate of a coral reef. *J Geophys Res*. <https://doi.org/10.1029/2006JC003770>
- Somero G (2015) Temporal patterning of thermal acclimation: from behavior to membrane biophysics. *J Exp Biol* 218:167–169
- Spencer Davies P (1989) Short-term growth measurement of corals using an accurate buoyant weighing technique. *Mar Biol* 101:389–395
- Stewart RIA, Dossena M, Bohan DA, Jeppesen E, Kordas RL, Ledger ME, Meerhoff N, Moss B, Mulder C, Shurin JB et al (2013) Mesocosm experiments as a tool for ecological climate-change research. *Adv Ecol Res* 48:71–181

**Publisher's Note** Springer Nature remains neutral with regard to jurisdictional claims in published maps and institutional affiliations.